

# Termination Kinetics of the Free-Radical Polymerization of Nonionized Methacrylic Acid in Aqueous Solution

Sabine Beuermann,<sup>†,§</sup> Michael Buback,<sup>\*,†</sup> Pascal Hesse,<sup>†</sup> Robin A. Hutchinson,<sup>\*,||</sup> Silvia Kukučková,<sup>†,‡</sup> and Igor Lacík<sup>‡</sup>

*Institute of Physical Chemistry, Georg-August-University, Tammannstraße 6, D-37077, Göttingen, Germany; Polymer Institute of the Slovak Academy of Sciences, Dúbravská cesta 9, 842 36, Bratislava, Slovak Republic; and Department of Chemical Engineering, Dupuis Hall, Queen's University, Kingston, Ontario K7L 3N6, Canada*

*Received December 30, 2007; Revised Manuscript Received February 25, 2008*

**ABSTRACT:** The termination kinetics of free-radical polymerization of nonionized methacrylic acid (MAA) in aqueous solution has been investigated at two MAA concentrations, 30 and 60 wt %, by single-pulse pulsed-laser initiated polymerization carried out in conjunction with  $\mu$ s time-resolved in-line monitoring of monomer conversion via near-infrared spectroscopy (SP–PLP–NIR). From measured values of  $k_t/k_p$  for 2000 bar, with the conversion-dependent propagation rate coefficient,  $k_p$ , being inferred from literature data, the chain-length-averaged termination rate coefficient,  $\langle k_t \rangle$ , is deduced as a function of monomer conversion,  $x$ . As with methyl methacrylate polymerization, the  $\langle k_t \rangle$  vs  $x$  dependence may be modeled under the assumption that, toward higher degrees of monomer conversion,  $\langle k_t \rangle$  is successively controlled by segmental diffusion, translational diffusion, and reaction diffusion. For 50 °C, 2000 bar, and initial monomer concentrations in water of 30 and 60 wt %, chemically initiated polymerizations have also been carried out. The resulting  $\langle k_t \rangle$  values are in good agreement with the data from SP–PLP–NIR.

## Introduction

The application of pulsed-laser polymerization (PLP) techniques has enormously improved the understanding of free-radical polymerization kinetics and mechanism during recent years. To measure propagation rate coefficients,  $k_p$ , the so-called PLP–SEC method is applied, which combines pulsed-laser initiated polymerization with polymer analysis by size-exclusion chromatography (SEC). The PLP–SEC technique was recommended as the method of choice for  $k_p$  determination by an IUPAC Working Party.<sup>1</sup> The initial focus of these PLP–SEC studies was on bulk homo and copolymerizations of oil-soluble monomers.<sup>2</sup> Recently, also aqueous-phase polymerizations of water-soluble monomers were investigated.<sup>3–12</sup> For the monomers studied in aqueous solution so far, a strong influence of monomer concentration on  $k_p$  was reported.<sup>3–12</sup> For example,  $k_p$  of nonionized MAA increases by more than 1 order of magnitude in passing from the bulk system to a highly dilute monomer solution.<sup>9,10</sup> The significant lowering in  $k_p$  is assigned essentially to a reduction in the Arrhenius pre-exponential factor,  $A(k_p)$ , resulting from the intermolecular interactions between the transition state (TS) structure for MAA propagation and an MAA environment being significantly stronger than the ones between this TS structure and an H<sub>2</sub>O environment. Thus in an MAA-rich environment, the barrier to rotational motion of the relevant degrees of motion of the TS structure experiences enhanced friction, which is associated with a lowering of the pre-exponential factor and thus of  $k_p$ .<sup>9</sup> The same trend of  $k_p$  being higher for lower initial monomer concentrations was found for *N*-isopropyl acrylamide,<sup>3</sup> acrylamide,<sup>8</sup> and acrylic acid<sup>4–6</sup> at their natural pH.

Data on termination rate coefficients,  $k_t$ , for radical polymerization in aqueous solution are scarce. Among the methods for deducing  $k_t$ , the SP–PLP–NIR technique is recommended

by the IUPAC Subcommittee on “Modeling polymerization kinetics and mechanism” as a powerful, although somewhat sophisticated and difficult method,<sup>13</sup> in which the monomer conversion induced by a single laser pulse (SP) is monitored via in-line near-infrared (NIR) spectroscopy with a time resolution of microseconds.<sup>14</sup> The primary experimental quantity is  $k_t/k_p$  which, with  $k_p$  being known from PLP–SEC, yields  $k_t$ . From several successive SP–PLP–NIR experiments carried out during a polymerization up to high degrees of monomer conversion,  $x$ , with each of them providing one  $k_t/k_p$  value,  $k_t$  may be determined as a function of  $x$ , provided that  $k_p$  is known for this conversion range. Propagation rate as a function of monomer conversion is not easily determined by PLP–SEC, as the application of this method is restricted to studies at low conversion. For aqueous MAA solutions, as has been noted above,  $k_p$  varies with the concentration of MAA monomer in the aqueous solution. As this concentration also changes during the course of a polymerization to high conversion,  $k_p$  may not be considered independent of conversion, as reasonably assumed for propagation in nonaqueous solutions.<sup>2</sup> Recent investigations into aqueous solution polymerizations with premixed poly(MAA), to mimic monomer conversion, revealed that it is the ratio of monomeric MAA to water in the polymerizing mixture consisting of monomer, polymer, and water which affects  $k_p$ , rather than the initial MAA concentration.<sup>12</sup> With the information on  $k_p$  being available for MAA polymerizations at various initial MAA concentrations and up to different degrees of monomer to polymer conversion,  $k_t$  may be derived via SP–PLP–NIR for aqueous-phase MAA polymerizations in an extended concentration and conversion range. The so-obtained  $k_t$  data will be compared with termination rate coefficients derived from chemically initiated polymerization. In case that the initiator decomposition rate coefficient,  $k_d$ , and the initiator efficiency,  $f$  (or the associated product,  $k_d f$ ), are known, chemically initiated polymerization yields  $k_t/k_p^2$  values, from which  $k_t(x)$  is estimated via the above-mentioned  $k_p(x)$  data.

\* Corresponding author.

<sup>†</sup> Institute of Physical Chemistry, Georg-August-University.

<sup>‡</sup> Polymer Institute of the Slovak Academy of Sciences.

<sup>§</sup> Current address: University of Potsdam.

<sup>||</sup> Department of Chemical Engineering, Dupuis Hall, Queen's University.

Within the first study into the termination kinetics in aqueous solution,  $k_t$  of 2-acrylamido-2-methylpropanesulfonic acid (AMPS) has been determined by a combination of SP–PLP–NIR and chemically initiated experiments, which yield  $k_t/k_p$  and  $k_t/k_p^2$ , respectively.<sup>15</sup> In addition to knowing  $k_d$  and  $f$ , for  $k_t/k_p^2$  determination, the estimate of individual rate coefficients from the two coupled parameters,  $k_t/k_p$  and  $k_t/k_p^2$ , further requires that the radical chain-length distributions in the instationary (SP–PLP) and stationary (chemically initiated) experiments are close to each other. The procedure of  $k_t$  determination via the two coupled parameters had to be selected, as with AMPS individual  $k_p$  was not accessible via PLP–SEC.

Methacrylic acid is perfectly suited for studies into the termination kinetics in aqueous solution, as PLP–SEC, SP–PLP–NIR, and chemically initiated experiments may be carried out, which allows for deducing  $k_t$  from two independent experiments, SP–PLP–NIR and chemically induced polymerization, both in conjunction with literature evidence on  $k_p$ . Moreover, MAA polymerization kinetics is much simpler than the one of acrylate-type monomers, such as acrylic acid (AA),<sup>4–7,16,17</sup> where inter- and intramolecular chain transfer results in the formation of midchain radicals<sup>18</sup> which leads to a rather complicated kinetic scheme with additional rate coefficients that are not easily accessible.<sup>19,20</sup>

We report data from SP–PLP–NIR experiments on aqueous MAA solutions with initial MAA concentrations of 3.50 and 7.09 mol·L<sup>−1</sup> (30 and 60 wt % MAA, respectively). To obtain reasonable signal-to-noise quality of the SP–PLP–NIR experiment, the polymerizations were carried out at a reaction pressure of 2000 bar. As the compressibility of the polymerizing systems is rather low, there is no reason to assume that high pressure affects the polymerization mechanism.<sup>2</sup> Chemically induced MAA polymerizations were also carried out at this high pressure. In both types of experiments, SP–PLP–NIR and chemically initiated polymerizations,  $k_t$  refers to a chain-length-averaged quantity, which is made clear by denoting the primary experimental quantities as  $\langle k_t \rangle/k_p$  and  $\langle k_t \rangle/k_p^2$ , respectively. It needs to be noted that the averaging of  $k_t$  occurs over different radical distributions: In the instationary SP–PLP–NIR experiment, termination occurs between radicals of almost identical size which linearly increases with time after applying the laser pulse (unless chain-transfer comes into play) whereas, in the stationary chemically initiated polymerizations, termination occurs between radicals of arbitrary size.<sup>1,15,21–23</sup>

## Experimental Section

**Chemicals.** Methacrylic acid (MAA, Fluka, > 98.0% stabilized with 0.025% hydroquinone monomethyl ether) was purified by passing through a column filled with inhibitor-remover (Aldrich). The photoinitiator 2,2-dimethoxy-2-phenyl acetophenone (DMPA, Aldrich, 99%) and the thermally decomposing initiator 2,2′-azobis (2-methylpropionamidine) dihydrochloride (V50, Fluka, ≥ 98%) were applied as received. Demineralized water was used to prepare the aqueous monomer solutions.

**Preparation of the Reaction Mixtures.** MAA, DMPA, and water were mixed in a 5 mL flask. Monomer concentrations were 3.50 and 7.09 mol·L<sup>−1</sup>, corresponding to 30 and 60 wt % MAA, respectively. An initial DMPA concentration of  $c_{\text{DMPA}} = 5 \text{ mmol} \cdot \text{L}^{-1}$  was mostly used. To remove oxygen, the monomer mixture was purged with nitrogen for 5 min. The solution was filled into the polymerization cell consisting of a Teflon tube closed by a cylindrical quartz window on each side. This internal cell was fitted into a stainless steel cell of transmission type equipped with two sapphire windows. Details of the experimental setup including heating and temperature control are given elsewhere.<sup>24</sup> For transmitting pressure on the internal cell, the autoclave was filled with *n*-heptane.

**SP–PLP–NIR Experiments.** The change in MAA concentration after applying a laser pulse was measured with a time resolution

of typically 10 μs. The SP–PLP–NIR setup consists of an excimer laser (Lextra 50, Lambda Physik) with a pulse width of 20 ns operated on the XeF-line at 351 nm, a 75 W tungsten halogen lamp (General Electric) powered by two batteries (12 V, 180 Ah), a BM 50 monochromator (B&M Spectronic), and a detector unit equipped with a fast InAs detector (EG & G, Judson) of 2 μs time resolution. The PC for data acquisition was equipped with a transient recorder card (16 bit TR 1621–4, Fast ComTec). The stainless steel cell is positioned between the tungsten lamp and the InAs detector.<sup>14</sup> The aqueous monomer-photoinitiator solution was irradiated with excimer laser light of 1 mJ energy per pulse. The pulse-induced decrease in monomer concentration is associated with an increase in transmitted light intensity at the characteristic monomer NIR peak position around 6173 cm<sup>−1</sup>. To improve signal-to-noise quality, up to four single pulse traces were coadded to obtain a monomer conversion vs time trace that is then subjected to kinetic analysis.

After carrying out several single-pulse experiments and covering a monomer conversion of about 5%, the stainless steel cell is inserted into the sample chamber of an FT-IR/NIR spectrometer (IFS 88, Bruker) to measure the full FT-NIR spectrum. Via such FT-NIR spectra, the light intensities at the monomer peak position, which are recorded as time-resolved voltage signals, are calibrated and converted into monomer concentration vs time  $t$  traces. The alternating sequence of time-resolved SP–PLP–NIR measurement at a fixed wavenumber and of FT-NIR detection of absolute MAA concentration via the full NIR spectrum is repeated unless the reaction mixture becomes inhomogeneous. Within the polymerizations at 30 wt % MAA, almost complete monomer conversion was reached.

**Chemically Initiated Polymerizations.** Monomer, V50, and water are mixed in a 5 mL flask and purged with nitrogen under ice cooling for three minutes. The mixture is filled into the internal cell, which is fitted into the stainless steel cell that has been preheated to the polymerization temperature. After applying pressure, the stainless steel cell is immediately inserted into the sample chamber of the FT-IR/NIR spectrometer and NIR spectra are taken until MAA conversion is complete. As detailed for the AMPS polymerizations in aqueous phase,<sup>15</sup> the first overtone of the C–H stretching vibration at the C=C double bond has been used to monitor MAA conversion as a function of polymerization time. Spectra were taken every 60 s. Polymerizations in aqueous solution of MAA were carried out at 50 °C and 2000 bar, as were the SP–PLP experiments, with initial V50 concentrations of 2.7, 1.1, and 0.55 mmol·L<sup>−1</sup>.

## Results and Discussion

**Generalized  $k_p$  Correlation.** The primary experimental results of instationary SP–PLP–NIR experiments and stationary chemically induced polymerizations are  $\langle k_t \rangle/k_p$  and  $\langle k_t \rangle/k_p^2$ , respectively. Thus, estimation of  $\langle k_t \rangle$  from those coupled parameters requires knowledge of the propagation rate coefficient at reaction conditions, that is temperature, pressure, initial monomer concentration and monomer to polymer conversion. To estimate  $k_p$  for different experimental conditions, the  $k_p$  dependencies need to be fitted to appropriate functional forms. Within our recent publication on the propagation rate of nonionized MAA,<sup>9</sup> it was shown that the temperature dependence of  $k_p$  is associated with an almost constant activation energy ( $15.6 \pm 1.1 \text{ kJ} \cdot \text{mol}^{-1}$ ) within wide ranges of monomer concentration, from 5 wt % MAA in water to bulk polymerization, which allows one to introduce one single temperature dependent parameter into the data fitting procedure. The propagation rate coefficient which was extrapolated to infinitely low monomer concentrations in water,  $k_{p,0}$ , was estimated as

$$k_{p,0}(T)/\text{L} \cdot \text{mol}^{-1} \cdot \text{s}^{-1} = 4.1 \times 10^6 \exp\left(-\frac{1.88 \times 10^3}{(T/K)}\right) \quad (1)$$

The decrease of  $k_p$  toward increased initial monomer concentration was implemented by fitting the experimental data to an exponential decay function which includes an offset

$$k_p(w_{\text{MAA}}^0, T) = k_{p,0}(A + (1 - A)\exp(-Bw_{\text{MAA}}^0)) \quad (2)$$

where  $W_{\text{MMA}}^0$  is the initial weight fraction of MAA in water and  $A$  and  $B$  are fit parameters. The values of  $A$  and  $B$  were adjusted to match the curvature of the experimental data in a plot of  $k_p/k_{p,0}$  vs  $W_{\text{MMA}}^0$ . The best representation of the experimental data was achieved for  $A = 0.08$  and  $B = 5.3$ . The  $k_p$  values for ambient pressure polymerizations of MAA in water at different polymerization temperatures are plotted against monomer weight fraction in Figure 1. The lines are estimates according to eq 2 using the parameters given above. The ordinate is plotted in logarithmic form in order to obtain a good visualization of the excellent agreement of the experimental data with the simple fit function and one single set of parameters  $A$  and  $B$ .

For additional implementation of the pressure dependence of  $k_p$ , data collected for polymerizations of 10, 30 and 60 wt % of MAA carried out at 25 °C and pressures ranging from 1 to 2000 bar<sup>25,26</sup> were analyzed. Linear regression of the variation of  $\ln(k_p)$  with pressure,  $p$ , results in a monomer-concentration-dependent activation volume of  $\Delta V^\ddagger(k_p) = -(8.0 + 9.0w_{\text{MAA}}^0) \text{ cm}^3 \cdot \text{mol}^{-1}$ . The extrapolated activation volume of  $-17.0 \text{ cm}^3 \cdot \text{mol}^{-1}$  for 100 wt % MAA ( $w_{\text{MAA}}^0 = 1$ ) is close to  $\Delta V^\ddagger(k_p) = -16.7 \text{ cm}^3 \cdot \text{mol}^{-1}$  determined for methyl methacrylate (MMA) bulk polymerization at 30 °C.<sup>27</sup> The origin of the significant reduction in the absolute value of  $\Delta V^\ddagger(k_p)$  toward lower MAA concentration in water is not yet clear. The general dependence of  $k_p$  on temperature, pressure, and initial weight fraction of monomer in water reads:

$$k_p(w_{\text{MAA}}^0, T, p) / \text{L} \cdot \text{mol}^{-1} \cdot \text{s}^{-1} = (3.3 \times 10^5 + 3.8 \times 10^6 \exp(-5.3w_{\text{MAA}}^0)) \times \exp\left(-\frac{1.88 \times 10^3 - (0.096 + 0.11w_{\text{MAA}}^0)(p/\text{bar})}{(T/\text{K})}\right) \quad (3)$$

This  $k_p$  correlation refers to the weight fraction of MAA in the initial polymerization period, where PLP–SEC experiments are generally performed. In order to estimate  $k_p$  as a function of monomer to polymer conversion, a series of PLP–SEC experiments has been carried out on systems with premixed poly(MAA).<sup>12</sup> The resulting data reveals that it is primarily the ratio of MAA monomer to water which determines  $k_p$ . Whether the MAA-in-water concentration is varied by selecting different initial MAA contents or by consuming monomer during

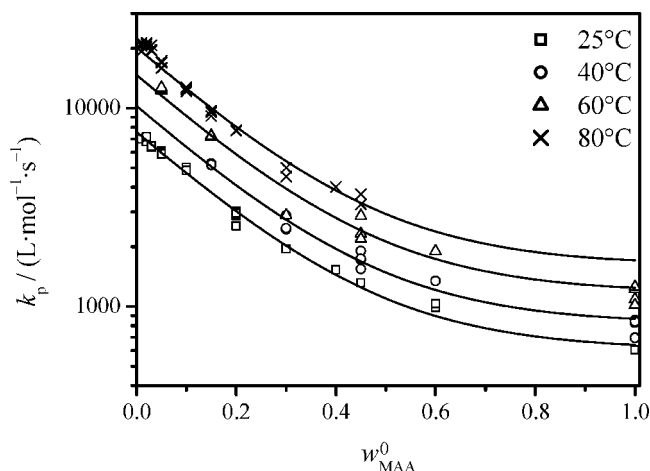


**Figure 1.** Dependence of the propagation rate coefficient,  $k_p$ , on the initial weight fraction of monomer in water,  $w_{\text{MAA}}^0$ , for polymerization of methacrylic acid in water at ambient pressure and different temperatures (data from ref 9). The full lines are best fits of the experimental data to eq 2 with the parameters  $A = 0.08$  and  $B = 5.3$ .

polymerization plays no major role. Eq 3 thus appears to be valid for any MAA weight fraction,  $w_{\text{MAA}}$ . Arbitrary  $w_{\text{MAA}}$  may be expressed by the initial weight fraction,  $w_{\text{MAA}}^0$ , and the degree of monomer conversion,  $x$ , according to eq 4:

$$w_{\text{MAA}} = \frac{w_{\text{MAA}}^0(1 - x)}{1 - w_{\text{MAA}}^0x} \quad (4)$$

It should be noted that the MAA weight fraction,  $w_{\text{MAA}}$ , in eq 4 is solely determined by the actual monomer and water concentrations. Poly(MAA) material is not included in the estimate of this weight fraction. Combination of eqs 3 and 4 yields eq 5, which has been applied for estimating  $k_p$  as a function of initial MAA concentration, of monomer conversion, and of temperature and pressure throughout the subsequent results and discussion section. The so-obtained  $k_p$  data were used to estimate  $\langle k_t \rangle$  from the primary experimental quantities,  $\langle k_t \rangle / k_p$  and  $\langle k_t \rangle / k_p^2$ , deduced from instationary SP–PLP–NIR experiments and stationary chemically induced polymerizations, respectively.

$$k_p(w_{\text{MAA}}^0, T, p, x) / \text{L} \cdot \text{mol}^{-1} \cdot \text{s}^{-1} = \left( 3.3 \times 10^5 + 3.8 \times 10^6 \exp\left(-\frac{5.3w_{\text{MAA}}^0(1 - x)}{1 - w_{\text{MAA}}^0x}\right) \right) \times \exp\left(-\frac{1.88 \times 10^3 - \left(0.096 + \frac{0.11w_{\text{MAA}}^0(1 - x)}{1 - w_{\text{MAA}}^0x}\right)(p/\text{bar})}{(T/\text{K})}\right) \quad (5)$$

**Determination of  $\langle k_t \rangle$  by SP–PLP–NIR.** Although being a nonideal photoinitiator, DMPA was used for the SP–PLP–NIR experiments rather than 2-methyl-4'-(methylthio)-2-morpholinopropiophenone (MMMP) which, in principle, is an ideal photoinitiator for SP–PLP studies, as both primary initiator-derived radicals are capable of efficiently starting chain growth.<sup>28</sup> However, MMMP could not be used because of poor solubility in MAA–water mixtures and side-reactions in protic solvents.<sup>29</sup> The two DMPA-derived primary radicals largely differ in their efficiency of starting chain growth. The benzoyl radical easily adds to monomer molecules, whereas the acetal radical primarily contributes to chain termination.<sup>30–32</sup> At low radical concentrations the impact of the poorly initiating primary radicals is, however, negligible and the resulting  $\langle k_t \rangle$  values are close to true average termination rate coefficients, although nonideal initiator behavior is neglected in the kinetic scheme used for data analysis.<sup>32</sup> The required low free-radical concentrations were chosen for the SP–PLP–NIR experiment by suitably selecting initiator concentration and laser pulse energy. For a detailed discussion of the influence of DMPA concentration on the obtained kinetic data, the reader is referred to refs 28 and 32.

As an example of primary experimental data from SP–PLP–NIR, the upper part of Figure 2 shows two MAA concentration vs time traces obtained during the course of an experiment with an initial MAA concentration of 60 wt %. Relative monomer concentration,  $c_{\text{M}}(t)/c_{\text{M}}^0$ , is plotted vs time  $t$  after applying the laser pulse at  $t = 0$ . Monomer conversion from preceding laser pulsing was 6.1% and 22.5%, respectively.  $c_{\text{M}}^0$  is the monomer concentration prior to laser pulsing at  $t = 0$ . The  $c_{\text{M}}^0$  value for a particular experiment is given by the initial monomer concentration (30 or 60 wt % MAA) and by the degree of overall MAA conversion,  $x$ , resulting from polymerization induced by preceding pulses. Upon applying the very first laser pulse to the system,  $c_{\text{M}}^0$  is identical to the preselected initial MAA concentration, which is either 30 or 60 wt %. During each polymerization, series of SP–PLP experiments are carried out. The horizontal pretrigger region in Figure 2 demonstrates that



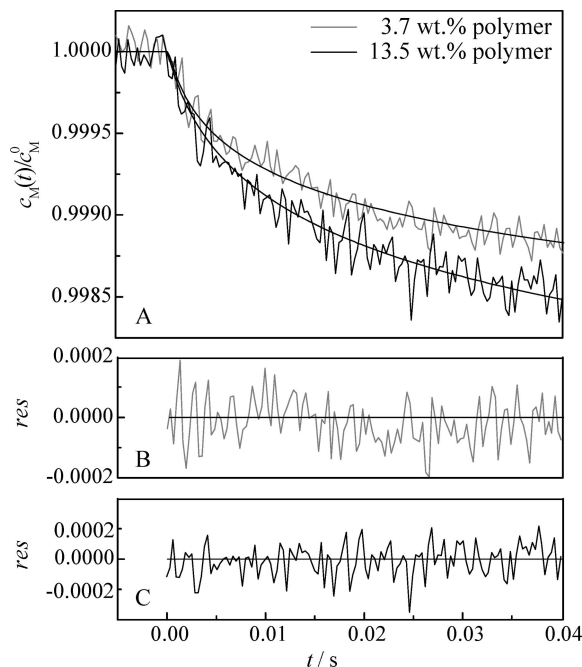


**Figure 2.** (A) Change in relative monomer concentration,  $c_M(t)/c_M^0$ , after applying an excimer laser pulse, at  $t = 0$ , during a methacrylic acid (MAA) polymerization at 50 °C and 2000 bar in aqueous solution with an initial monomer concentration of 60 wt % MAA. At  $t = 0$ , when the laser pulse is applied, the poly(MAA) content from preceding polymerization is 3.7 or 13.5 wt % (6.1 and 22.5% of monomer to polymer conversion, respectively). (B and C) Differences between measured data and the ones fitted to eq 6 are illustrated by the plot of residuals ( $res$ ) in the lower part of the figure, where parts B and C refer to experiments carried out at overall MAA conversions of 6.1 and 22.5%, respectively.

polymerization induced by preceding pulses has ceased. At 0.04 s after firing the laser pulse, relative MAA concentration,  $c_M(t)/c_M^0$ , has decreased by about 0.11% within the SP–PLP–NIR experiment carried out at  $x = 0.061$ , that is at a poly(MAA) fraction of 3.7 wt %. At a later stage during the same polymerization reaction, at a polymer weight fraction of 13.5 wt % ( $x = 0.225$ ), a single laser pulse induces a change in  $c_M(t)/c_M^0$  by 0.15% between  $t = 0$  and 0.04 s.

The concentration vs time traces in Figure 2 were fitted to eq 6 which refers to ideal single pulse kinetics with reference to the termination rate law:  $r_t = -2k_t c_R^2$ .<sup>2</sup> In systems where chain transfer is negligible, termination in SP–PLP experiments occurs between two radicals of almost identical length  $i$ , where  $i$  increases linearly with time  $t$  after applying the laser pulse at  $t = 0$ . To indicate that termination kinetics is chain-length dependent,  $k_t$  in eq 6 has been replaced by  $\langle k_t \rangle$ . The expression for the change of relative monomer concentration with time  $t$  after the laser pulse reads

$$\frac{c_M(t)}{c_M^0} = (2\langle k_t \rangle c_R^0 t + 1)^{-k_p/2\langle k_t \rangle} \quad (6)$$

where  $c_R^0$  is the concentration of primary radicals generated by instantaneous laser-induced decomposition of the photoinitiator. Fitting of experimental monomer concentration vs time traces yields  $k_p/\langle k_t \rangle$  and  $\langle k_t \rangle c_R^0$ . If either  $k_p$  or  $c_R^0$  are known, individual  $\langle k_t \rangle$  values may be calculated from  $k_p/\langle k_t \rangle$  or  $\langle k_t \rangle c_R^0$ , respectively. Mostly,  $k_p$  is accessible from PLP–SEC experiments, for which reason the coupled parameter  $\langle k_t \rangle/k_p$  is of particular interest.

The fits to eq 6 of the measured MAA conversion vs time data (Figure 2) allow for an excellent representation of the experimental data, as is also demonstrated by the plots of residuals in the lower part of Figure 2. The time interval up to

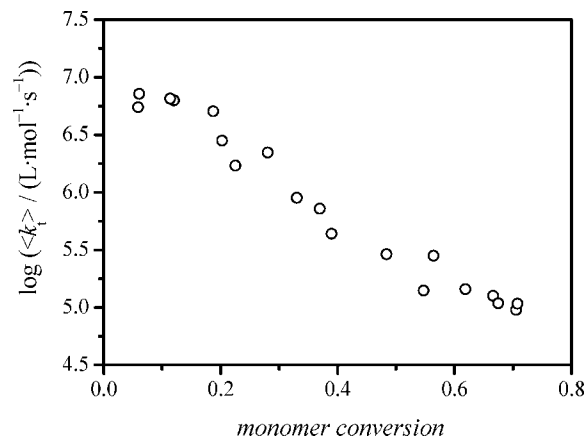


**Figure 3.** Dependence of the termination rate coefficient,  $\langle k_t \rangle$ , on monomer conversion, for a methacrylic acid polymerization in aqueous solution (60 wt % MAA) at 50 °C and 2000 bar. The photoinitiator concentration in the SP–PLP experiment was  $c_{DMPA} = 5 \times 10^{-3} \text{ mol} \cdot \text{L}^{-1}$ .  $\langle k_t \rangle$  was calculated from  $\langle k_t \rangle/k_p$  by using the  $k_p$  expression given in eq 5.

0.04 s refers to the range in which chain length  $i$  increases up to approximately 1000.<sup>33</sup> SP–PLP–NIR traces measured at the lower MAA concentration of 30 wt % are equally well fitted to eq 6. Thus, each of the two signals in Figure 2A may be adequately represented by one  $\langle k_t \rangle$  value, although a wide range of radical chain lengths is covered within both  $c_M(t)/c_M^0$  vs time traces. As discussed elsewhere,<sup>15</sup> the remarkable quality of the data fit to eq 6 is not indicative of  $k_t$  being independent of chain length, but is a specific feature of DMPA acting as the photoinitiator. There is partial compensation of the effects due to chain-length dependent  $k_t$  and to primary radical termination of the poorly initiating acetal fragment. The conversion vs time traces measured on the aqueous MAA solutions are evaluated according to ideal polymerization kinetics and the resulting rate coefficient is referred to as  $\langle k_t \rangle$  in order to indicate that the so-obtained value is an average over chain-length-dependent  $k_t$  values. The same approach has been used in the analysis of the SP–PLP–NIR experiments on aqueous solutions of AMPS.<sup>15</sup>

The variation of  $\langle k_t \rangle$  with monomer conversion, as obtained via fitting of SP–PLP–NIR traces to eq 6 and implementing  $k_p$  according to eq 5, is plotted in Figure 3 for an aqueous-phase MAA polymerization at 50 °C and 2000 bar. The initial MAA concentration was 60 wt %. Data could be measured up to 70% MAA conversion before the reaction mixture turned heterogeneous. Within the experiment carried out on the solution with an initial concentration of 30 wt % of MAA, even 90% monomer conversion could be reached. In the initial reaction period (Figure 3) an approximately constant value of  $\langle k_t \rangle$  is found. Above  $x = 0.20$ ,  $\langle k_t \rangle$  decreases significantly, by around 1.5 orders of magnitude up to  $x = 0.50$ . Such significant changes of  $\langle k_t \rangle$  are typical for methacrylate monomers with small and medium-size alkyl ester side chain, such as methyl methacrylate<sup>2,34,35</sup> and butyl methacrylate.<sup>36</sup>

The  $\langle k_t \rangle$  vs  $x$  dependence in Figure 3 may be understood by assuming control of termination by segmental diffusion (SD), translational diffusion (TD), and reaction diffusion (RD). At low conversion,  $\langle k_t \rangle$  is determined by SD, which refers to the orientational motion of two coiled macroradicals by which the radical functionalities approach each other sufficiently closely to allow for immediate termination. Increasing monomer conversion is associated with an increase in bulk viscosity. As a consequence, translational (center-of-mass) diffusion may become rate determining. The data in Figure 3 indicate that  $\langle k_t \rangle$  runs under control by TD at about  $x = 0.20$ . The pronounced decrease in  $\langle k_t \rangle$  up to  $x = 0.50$  reflects the reduced translational

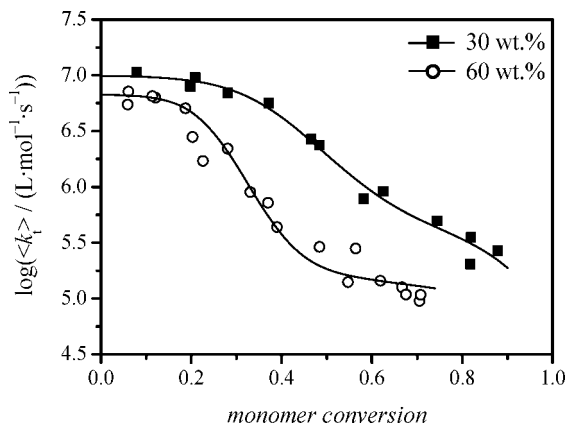


**Figure 4.** Conversion dependence of the chain-length averaged termination rate coefficient,  $\langle k_t \rangle$ , for methacrylic acid polymerizations at 50 °C, 2000 bar, and initial monomer concentrations of 30 and 60 wt % MAA, respectively.  $\langle k_t \rangle$  was calculated from  $\langle k_t \rangle/k_p$  by using the  $k_p$  expression given in eq 5. The lines are fits of the experimental data to eq 7. The associated parameter values are listed in Table 1.

mobility of the macroradicals at significantly increasing bulk viscosity. At even higher degrees of monomer conversion, the lowering of  $\langle k_t \rangle$  with  $x$  is less pronounced, an observation that indicates that  $\langle k_t \rangle$  becomes controlled by reaction diffusion.<sup>37</sup> This mechanism has been thoroughly discussed for the bulk homopolymerizations of ethene and butyl acrylate.<sup>38,39</sup> Control of  $\langle k_t \rangle$  by reaction diffusion suggests that the motion of the radical functionality essentially occurs via propagation steps of the dangling free-radical chain end. Equation 7 was introduced to model  $\langle k_t \rangle$  for polymerizations where the three types of diffusion control (SD, TD, and RD) are operating:<sup>38</sup>

$$\langle k_t \rangle = \frac{1}{k_{SD}^{-1} + \eta_r/k_{TD}^0} + C_{RD}(1-x)k_p \quad (7)$$

The first term on the right-hand side of eq 7 represents the contributions of translational and segmental diffusion to overall termination.  $k_{SD}$  is the rate coefficient of segmental diffusion. This coefficient is assumed to be independent of monomer conversion and thus of polymer content, as the segmental reorientation process is envisaged to take place within two coiled macroradicals.  $k_{TD}^0$  is the translational diffusion rate coefficient at zero conversion and  $\eta_r$  is the relative bulk viscosity,  $\eta_r = \eta/\eta_0$ , where  $\eta_0$  denotes the viscosity of the reaction mixture prior to polymerization, but at polymerization temperature and pressure. The second term on the rhs of eq 7 accounts for the reaction diffusion contribution to overall  $\langle k_t \rangle$ , with  $C_{RD}$  being the reaction diffusion constant, and  $k_p$  varying with conversion as described by eq 5. At very high conversions even  $k_p$  may run under diffusion control. This effect is not considered in eq 7, but is contained in the associated general expression.<sup>38</sup>

Plotted in Figure 4 are the  $\langle k_t \rangle$  values for polymerizations of 30 and 60 wt % MAA in water at 50 °C and 2000 bar which are obtained from  $\langle k_t \rangle/k_p$  using the  $k_p$  correlation given in eq 5. For 30 wt % MAA, the initial plateau value of  $\langle k_t \rangle$  is slightly above the one for 60 wt % and extends up to higher degrees of monomer conversion. After passing the initial plateau region,  $\langle k_t \rangle$  decreases significantly, by about 1.5 orders of magnitude between 20 and 50% conversion with the 60 wt % MAA system and by about 1 order of magnitude between 30 and 60% conversion with the 30 wt % MAA system. Toward even higher degrees of monomer conversion, the decrease in  $\langle k_t \rangle$  becomes less pronounced. This effect is clearly seen with the polymerization of the 60 wt % MAA solution.

The lines in Figure 4 are representations of the experimental data by eq 7. The associated parameter values are listed in Table

**Table 1. Model Parameters Used for Fitting the Experimental Data in Figure 4 to eq 7<sup>a</sup>**

$c_{MAA}/\text{wt } \%$	30	60
$k_{SD}/\text{L} \cdot \text{mol}^{-1} \cdot \text{s}^{-1}$	$(9.3 \pm 0.2) \times 10^6$	$(6.5 \pm 0.2) \times 10^6$
$C_\eta$	$12.8 \pm 0.4$	$21.2 \pm 0.7$
$k_{TD}^0/\text{L} \cdot \text{mol}^{-1} \cdot \text{s}^{-1}$	$1.0 \times 10^9$	$1.0 \times 10^9$
$C_{RD}$	$94 \pm 11$	$61 \pm 7$

<sup>a</sup> The parameter values refer to MAA polymerization at 50 °C and 2000 bar. For further details, see the text.

1.  $k_{SD}$  is obtained as the value of experimental  $\langle k_t \rangle$  in the very initial polymerization period.  $k_{TD}^0 = 1.0 \times 10^9 \text{ L} \cdot \text{mol}^{-1} \cdot \text{s}^{-1}$  has been adopted from studies into alkyl methacrylate termination rate which report monomer concentration independent  $k_{TD}^0$  values of this order of magnitude.<sup>35</sup> The rate coefficient of translation diffusion during polymerization,  $k_{TD}$ , is given by  $k_{TD}^0/\eta_r$ . Bulk viscosity depends on the characteristics of each individual polymerization reaction, in particular on the polymer content, that is on the degree of monomer conversion,  $x$ , and on the type of polymer produced, e.g., whether low-molecular or high-molecular weight material is formed. Usually, information on  $\eta_r$  is not available. Within preceding studies into bulk (meth)acrylate<sup>38</sup> and MMA solution polymerizations,<sup>35</sup> as a rough approximation for modeling the conversion dependence of relative bulk viscosity,  $\eta_r(x)$ , eq 8 has been used:

$$\ln \eta_r = C_\eta x \quad (8)$$

The parameter  $C_\eta$  may be looked upon as an adjustable parameter, which essentially determines the conversion dependence of  $\langle k_t \rangle$  under conditions where  $k_{TD}$  controls termination rate. The  $C_\eta$  parameters in Table 1 may be found from the slope of the straight line which intersects the ordinate at  $\log(k_{TD}^0)$  and passes through the inflection point of the sigmoidal  $\log(\langle k_t \rangle)$  vs  $x$  curve, that is in the region where  $k_{TD}$  controls termination rate but was simultaneously determined with  $C_{RD}$  via fitting of  $\langle k_t \rangle$  data according to eq 7. The so-obtained  $C_\eta$  values are 12.8 and 21.2 for the polymerizations of 30 and 60 wt % MAA, respectively. The roughly 2-fold higher value of  $C_\eta$  at 60 wt % MAA as compared to the system with 30 wt % MAA may be understood as being due to twice the amount of polymer being present at identical monomer conversion. Linear extrapolation of  $C_\eta$  toward  $w_{MAA}^0 = 0$  yields a  $C_\eta$  value close to zero which corresponds to constant  $\eta_r$  as is to be expected in the hypothetical case of no monomer being present and thus no polymerization taking place. The clear trend of decreasing  $C_\eta$  toward lower monomer concentration has also been seen with MMA solution polymerizations.<sup>35</sup> Extrapolation of  $C_\eta$  from this earlier study to zero monomer content however does not yield  $C_\eta$  close to zero, which may be due to the rather weak decrease of  $\langle k_t \rangle$  in the TD-controlled regime with MMA solution polymerizations and the associated significant error in deducing  $C_\eta$ . For bulk MAA polymerization a  $C_\eta$  value of about 35 is estimated from the 30 and 60 wt % data. This value is significantly above  $C_\eta = 21$  as obtained for MMA bulk polymerization.<sup>35</sup> The very pronounced increase of  $\eta_r$  with MAA bulk polymerization may be due to the action of strong hydrogen bonds which are absent with MMA. Moreover, differences in molecular weight distribution of the background polymer matrix may affect  $C_\eta$ . It goes without saying that one individual  $C_\eta$  value cannot fully take into account both polymer content and polymer size distribution of the reacting systems. It should further be noted that the size of  $C_\eta$  is affected by the selection of  $w_{MAA}^0$ . E.g., assuming  $k_{TD}^0$  at 60 wt % MAA to differ from the associated value for 30 wt % MAA by the same factor as do the associated  $k_{SD}$  values, yields an optimum fit of the  $\langle k_t \rangle$  vs  $x$  data with  $C_\eta = 20.0$  rather than with  $C_\eta = 21.2$ , as listed in Table 1.

The second adjustable parameter in the fitting procedure, the reaction diffusion constant, is listed as the last entry in Table 1.

For 60 wt % MAA,  $C_{RD}$  is obtained with a better accuracy, as the reaction diffusion controlled region is more pronounced than for 30 wt % MAA. The  $C_{RD}$  values in Table 1 are close to the numbers reported for MMA bulk polymerization at 60 °C:  $C_{RD} = 76$  at 1000 bar and  $C_{RD} = 50$  at 2000 bar.<sup>40</sup> That  $C_{RD}$  for polymerization of MAA in aqueous solution slightly decreases with increasing MAA concentration is in line with the argument used to describe the dependence of  $k_p$  on MAA content.<sup>9</sup> The stronger intermolecular hydrogen-bonded interactions at higher MAA content should enhance both the friction experienced by the transition state for propagation, which effect reduces  $k_p$ , and the friction which the free-radical chain ends experience during the reaction-diffusion process. A lower mobility of the macroradical chain-end should result in a lower  $C_{RD}$ .<sup>15,39</sup>

The parameters in Table 1 afford for an excellent representation of the experimental  $\langle k_t \rangle$  over a wide range of MAA conversion (Figure 4). This finding suggests that eq 7, which has been used for fitting  $\langle k_t \rangle$  of various monomers in both bulk and in organic solvents,<sup>2,36,38,39</sup> is applicable also toward radical polymerizations in aqueous solution. The variation of the parameters  $k_{SD}$  and  $C_\eta$  with solvent content seen in aqueous solution of MAA is consistent with what has been seen, e.g., for MMA polymerized in solution of toluene. The initial  $k_{SD}$  plateau value is slightly enhanced toward lower monomer content whereas, within the range of translational diffusion control, the  $\langle k_t \rangle$  vs  $x$  correlation is strongly affected by the solvent content.<sup>35</sup>

As mentioned above, the increase of  $C_\eta$  toward higher initial monomer concentration may be due to higher amounts of polymer being present at a given conversion. The approximately 2-fold increase of  $C_\eta$  between 30 and 60 wt % MAA implies that, for estimating the viscosity change during polymerization, a parameter  $C_\eta^*$  should be used which scales with polymer weight fraction  $w_{pMAA} = w_{MAA}x$ . Thus a modified expression (eq 9) may be used for fitting the experimental  $\langle k_t \rangle$  data measured on 30 and 60 wt % MAA in aqueous solution. As the variation of both  $k_{SD}$  and  $C_{RD}$  is minor as compared to the differences in translational diffusion behavior, expressed by  $C_\eta$ , for both MAA contents a single mean value of  $k_{SD}^*$  and of  $C_{RD}^*$  has been used within the fitting procedure. Equation 9 reads:

$$\langle k_t \rangle = \frac{1}{1/k_{SD}^* + \exp(C_\eta^* w_{MAA}^0 x)/k_{TD}^0} + C_{RD}^* (1-x) k_p \quad (9)$$

with the following mean values:  $k_{SD}^* = 7.9 \times 10^6 \text{ L} \cdot \text{mol}^{-1} \cdot \text{s}^{-1}$ ,  $C_{RD}^* = 77.5$ , and  $C_\eta^* = 39$ . The remarkably good representation of the experimental  $\langle k_t \rangle$  data (full line for 30 wt % and dashed line for 60 wt %) by eq 9 is illustrated by the plot of  $\log \langle k_t \rangle$  vs polymer weight fraction in Figure 5. The data from experiments at initial MAA concentrations of 30 and 60 wt % almost sit on top of each other, which indicates the general type of  $\langle k_t \rangle$  behavior. For an even more accurate representation of  $\langle k_t \rangle$  within extended ranges of MAA concentration, the experimental  $k_{SD}$  and  $C_{RD}$  values may be used for interpolation and extrapolation of  $k_{SD}$  and  $C_{RD}$  data for a given MAA weight fraction.

**Determination of  $\langle k_t \rangle$  by Chemically Initiated Polymerizations.** Chemically initiated (CI) polymerization under steady-state conditions provides access to  $\langle k_t \rangle/k_p^2$  in case that the initiator decomposition rate coefficient,  $k_d$ , and initiator efficiency,  $f$ , which represents the fraction of primary radicals from initiator decomposition that start chain growth, or the product of both quantities,  $k_d f$ , are known. Carrying out both CI and SP-PLP experiments, with  $k_p$  being available from PLP-SEC, allows for estimating  $\langle k_t \rangle$  as a function of monomer conversion from the two independent experiments. The CI polymerizations for MAA were performed at 50 °C, 2000 bar, and at MAA contents of 30 and 60 wt % in water as were the SP-PLP-NIR experiments. Monomer conversion was monitored via in-line FT-NIR spectroscopy. Monomer conversion vs reaction time,

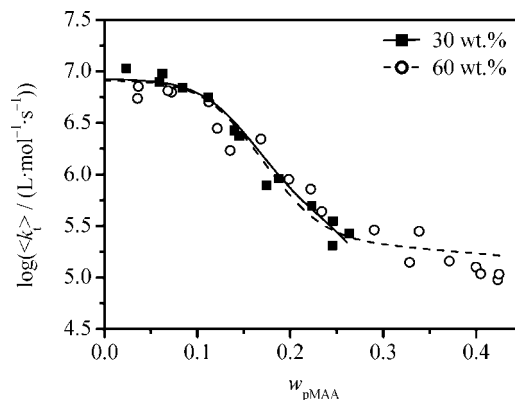


**Figure 5.** Dependence of the chain-length averaged termination rate coefficient,  $\langle k_t \rangle$ , on weight fraction of polymer,  $w_{pMAA}$ , for methacrylic acid polymerizations at 50 °C, 2000 bar and initial monomer concentrations of 30 and 60 wt % MAA, respectively. The lines are representations of the experimental data via eq 9 (full line for 30 wt % MAA and dashed line for 60 wt % MAA). The associated parameter values are listed in the text.

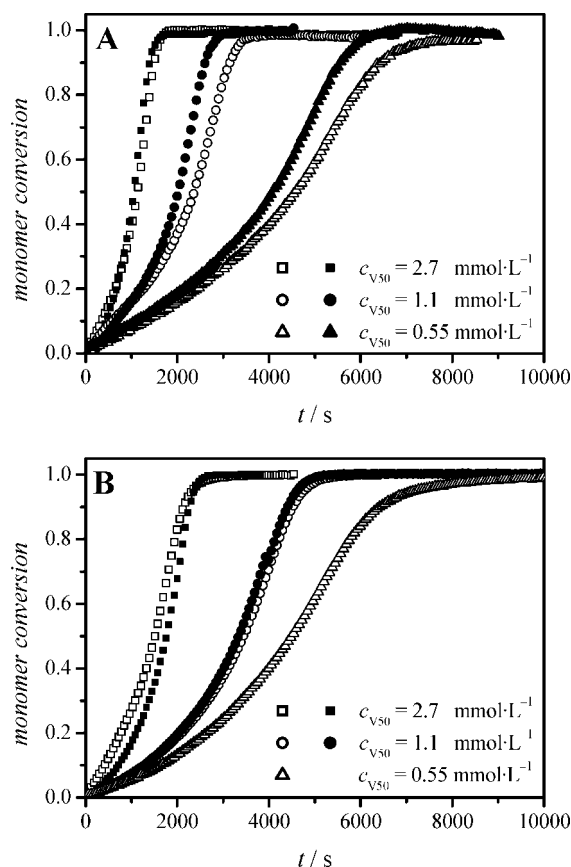


**Figure 6.** Monomer conversion vs time plots for chemically initiated polymerizations of 30 (A) and 60 wt % (B) of methacrylic acid in aqueous solution at 50 °C and 2000 bar. The primary initiator concentrations were 2.7, 1.1, and 0.55  $\text{mmol} \cdot \text{L}^{-1}$  of V50, respectively. Open and filled symbols refer to repeat experiments under ostensibly the same conditions.

$t$ , profiles deduced from FT-NIR are depicted in Figure 6A for 30 wt % of MAA and in Figure 6B for 60 wt % of monomer.

In most cases, duplicate experiments have been carried out. The agreement of polymerization data from measurements under ostensibly the same conditions is rather satisfactory, in particular in case of higher MAA concentration (Figure 6B) and of higher initiator concentration. The reasons behind these observations are the better quality of NIR analysis at higher MAA content and the



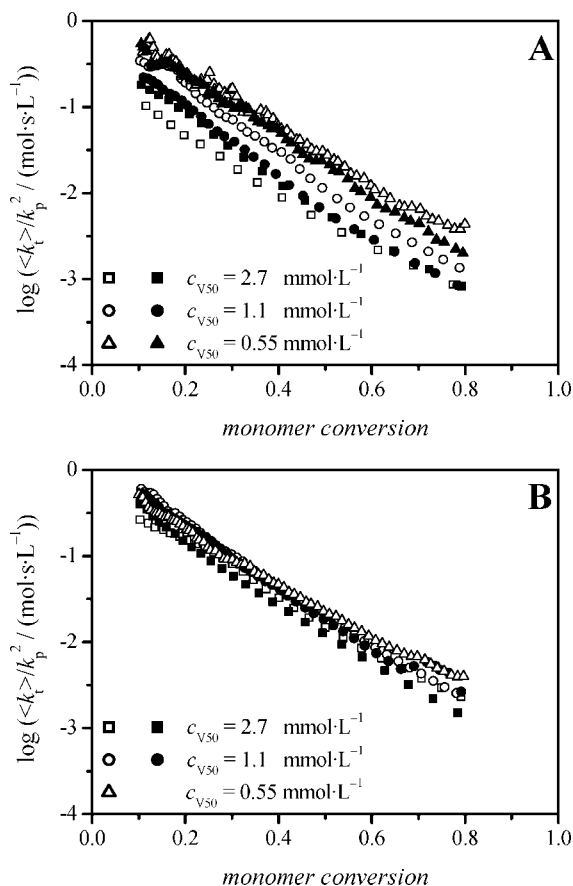


**Figure 7.** Conversion dependence of  $\langle k_t \rangle / k_p^2$  derived from chemically initiated polymerizations of 30 wt % (A) and 60 wt % (B) methacrylic acid in aqueous solution at 50 °C, 2000 bar with primary initiator concentrations of  $c_{V50} = 2.7, 1.1$ , and  $0.55 \text{ mmol} \cdot \text{L}^{-1}$ .

lower impact of impurities at high levels of radical concentration, respectively. A significant increase of the rate of polymerization,  $R_p$ , is seen toward higher initiator concentration.

The kinetic data in Figure 6 were analyzed via the expression for steady-state polymerization (eq 10):

$$R_p = -\frac{dc_M}{dt} = \frac{k_p}{\langle k_t \rangle^{0.5}} f^{0.5} k_d^{0.5} c_M c_I^{0.5} \quad (10)$$

with the initiator concentration  $c_I$ .

The reported ambient-pressure decomposition rate coefficient of V50 in aqueous solution at 50 °C,  $k_d = 8.14 \times 10^{-6} \text{ s}^{-1}$ , has been adopted to hold for 2000 bar, as has been the reported ambient-pressure initiator efficiency,  $f = 1.41$ . Polymerization rate,  $R_p = -dc_M/dt$ , was estimated from first-derivative curves of  $c_M$  vs  $t$  traces determined via Origin 6.1 with subsequent smoothing. Plotted in Figure 7 are the  $\langle k_t \rangle / k_p^2$  vs  $x$  values obtained, via eq 10, from  $R_p$  of the chemically initiated polymerizations at 30 and 60 wt % MAA in aqueous solution for 50 °C/2000 bar and from the known values of  $f$ ,  $k_d$ ,  $c_I$ , and  $c_M$ . The data are plotted only up to 80% monomer conversion, as the minor changes of  $c_{MAA}$  with time at higher conversions induce a significant scatter for  $\langle k_t \rangle / k_p^2$ . As inhibition may significantly affect  $\langle k_t \rangle / k_p^2$  in the early polymerization period, values for conversions below 10% were also ignored; the initiator consumed during this period is accounted for in the estimation of  $\langle k_t \rangle / k_p^2$  by eq 10. A close overlap of the entire data set for polymerizations at 60 wt % initial MAA concentration is seen, whereas  $\langle k_t \rangle / k_p^2$  for 30 wt % MAA slightly increases toward lower V50 concentration. The origin of the increase in  $\langle k_t \rangle / k_p^2$ , by about half an order of magnitude in passing from

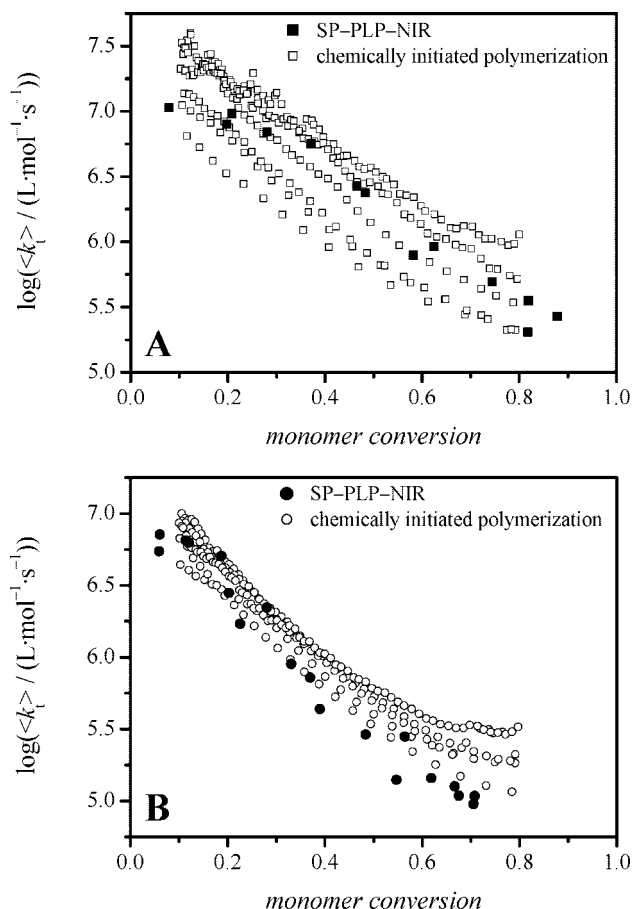


**Figure 8.** Conversion dependence of  $\langle k_t \rangle$  derived from chemically initiated polymerizations of 30 wt % (A) and 60 wt % (B) methacrylic acid in aqueous solution at 50 °C, 2000 bar with V50 concentrations of 2.7, 1.1 and  $0.55 \text{ mmol} \cdot \text{L}^{-1}$  (open symbols). The  $\langle k_t \rangle$  data from SP-PLP-NIR at identical monomer concentration are given as filled symbols.  $\langle k_t \rangle$  values are calculated from  $\langle k_t \rangle / k_p^2$  or  $k_t / k_p$  using the general  $k_p$  expression given by eq 5.

2.7 to  $0.55 \text{ mmol} \cdot \text{L}^{-1}$  initiator, is not clear. Probably, a loss of initiator-derived radicals due to inhibition results in a lower than expected radical concentration which, by the evaluation procedure, translates into termination rate coefficients that are too large. For both 30 and 60 wt % of MAA in aqueous solution, a pronounced decrease of the coupled parameter  $\langle k_t \rangle / k_p^2$  is seen toward higher conversions.

Figure 8 shows a comparison of  $\langle k_t \rangle$  values for 30 (A) and 60 wt % (B) of MAA in aqueous solution at 50 °C and 2000 bar as obtained from both stationary (open symbols) and instationary (filled symbols) experiments.  $\langle k_t \rangle$  was extracted from the two types of coupled parameters via  $k_p$  values estimated from eq 5. For 30 wt % of MAA, the  $\langle k_t \rangle$  data from SP-PLP-NIR fit into the range of  $\langle k_t \rangle$  values provided by the data from CI polymerizations performed at different initiator concentrations. The  $\langle k_t \rangle$  data for aqueous solutions with an initial MAA content of 60 wt % demonstrate the satisfactory agreement of  $\langle k_t \rangle$  data from SP-PLP and from CI polymerization. A sigmoidal curvature cannot be clearly detected from the  $\langle k_t \rangle$  vs monomer conversion data obtained by CI polymerization. There is, however, a weak indication with some of the 60 wt % MAA data that the decrease of  $\langle k_t \rangle$  with conversion appears to be somewhat weaker in both the low and high conversion regions. The comparison of stationary and instationary experiments suggests that the SP-PLP-NIR experiments allow for a more detailed and accurate study into the termination kinetics than do the CI polymerization experiments, e.g., the sigmoidal  $\langle k_t \rangle$

vs  $x$  curvature, which is what one expects from a comparison with MMA polymerization data, can be clearly seen from SP–PLP.

The enhanced scattering and the systematic shift with initiator concentration of the  $\langle k_t \rangle$  data from CI polymerization may be due to an impact of inhibition and thus of impurities on the kinetic data, which is not easily avoidable in CI polymerization, but can be overcome by the intense laser pulsing where the first few pulses may have some cleaning effect on the system. The chain-length distribution being broader in CI polymerizations may give rise to some smoothing of  $\langle k_t \rangle$  vs  $x$  data. With the SP–PLP experiments, on the other hand, the chain-length distribution is very narrow, which facilitates detection of conversion-related effects on  $\langle k_t \rangle$ .

In view of the various sources of error that should primarily affect CI polymerizations rather than SP–PLP experiments, the agreement of absolute  $\langle k_t \rangle$  values obtained by the two methods must be considered as very satisfactory. For an inspection of detailed effects associated with the mode of diffusion control of  $\langle k_t \rangle$  it appears recommendable to apply the SP–PLP–NIR method rather than carrying out stationary CI polymerization experiments.

The satisfactory agreement of  $\langle k_t \rangle$  values derived from chemically initiated polymerizations and SP–PLP–NIR further indicates that combination of experimental  $\langle k_t \rangle/k_p$  and  $\langle k_t \rangle/k_p^2$  values should yield reliable individual rate coefficients of propagation and termination for MAA in aqueous solution. This procedure has already been used within our recent study into aqueous-solution polymerization of AMPS.<sup>15</sup>

## Conclusions

Termination rate coefficients for MAA polymerizations in aqueous solution were determined by the SP–PLP–NIR method at two initial monomer concentrations, of 30 and 60 wt %. For extraction of  $\langle k_t \rangle$  from the primary experimental  $\langle k_t \rangle/k_p$  data, a correlation of  $k_p$  with temperature, pressure, initial monomer concentration and monomer to polymer conversion was established. The conversion dependence of  $\langle k_t \rangle$  exhibits the same trends as observed for polymerizations of methacrylic acid esters: At low conversion,  $\langle k_t \rangle$  is controlled by segmental diffusion. At intermediate conversions, translational diffusion becomes rate determining. Indications of control by reaction diffusion are seen at the highest degrees of monomer conversion. Upon lowering the water content of the polymerizing mixture, the transition from segmental diffusion to translational diffusion is shifted to lower monomer conversion and the decrease of  $\langle k_t \rangle$  under translational diffusion control is more pronounced as a consequence of the larger amount of polymer being present. The termination rate coefficient data for the two initial monomer concentrations under investigation closely overlap when plotted against the weight fraction of polymer. For comparison purposes, also CI stationary polymerization experiments have been carried out. The satisfactory agreement of  $\langle k_t \rangle$  vs monomer conversion data from SP–PLP–NIR and from CI polymerization indicates that combination of these two methods may be used for estimating individual propagation and termination rate coefficients. The quality of  $\langle k_t \rangle$  data from SP–PLP–NIR is superior over the one from the CI polymerization method.

**Acknowledgment.** P.H. acknowledges a fellowship by the *Fonds der Chemischen Industrie*. Financial support and a fellowship for S.K. by the Deutsche Forschungsgemeinschaft within the framework of the European Graduate School “Microstructural Control in Free Radical Polymerization” and financial support by BASF AG are gratefully appreciated.

## References and Notes

- (1) Buback, M.; Gilbert, R. G.; Russell, G. T.; Hill, D. J. T.; Moad, G.; O'Driscoll, K. F.; Shen, J.; Winnik, M. A. *J. Polym. Sci., Polym. Chem. Ed.* **1992**, *30*, 851–863.
- (2) Beuermann, S.; Buback, M. *Prog. Polym. Sci.* **2002**, *27*, 191–254.
- (3) Ganachaud, F.; Balic, R.; Monteiro, M. J.; Gilbert, R. G. *Macromolecules* **2000**, *33*, 8589–8596.
- (4) Kuchta, F.-D.; van Herk, A. M.; German, A. L. *Macromolecules* **2000**, *33*, 3641–3649.
- (5) Lacík, I.; Beuermann, S.; Buback, M. *Macromolecules* **2001**, *34*, 6224–6228.
- (6) Lacík, I.; Beuermann, S.; Buback, M. *Macromolecules* **2003**, *36*, 9355–9363.
- (7) Lacík, I.; Beuermann, S.; Buback, M. *Macromol. Chem. Phys.* **2004**, *205*, 1080–1087.
- (8) Seabrook, S. A.; Tonge, M. P.; Gilbert, R. G. *J. Polym. Sci., Polym. Chem. Ed.* **2005**, *43*, 1357–1368.
- (9) Beuermann, S.; Buback, M.; Hesse, P.; Lacík, I. *Macromolecules* **2006**, *39*, 184–193.
- (10) Beuermann, S.; Buback, M.; Hesse, P.; Kuchta, F.-D.; Lacík, I.; van Herk, A. M. *Pure Appl. Chem.* **2007**, *79*, 1463–1469.
- (11) Beuermann, S.; Buback, M.; Hesse, P.; Kukčková, S.; Lacík, I. *Macromol. Symp.* **2007**, *248*, 23–32.
- (12) Beuermann, S.; Buback, M.; Hesse, P.; Kukčková, S.; Lacík, I. *Macromol. Symp.* **2007**, *248*, 41–49.
- (13) Barner-Kowollik, C.; Buback, M.; Egorov, M.; Fukuda, T.; Goto, A.; Olaj, O. F.; Russell, G. T.; Vana, P.; Yamada, B.; Zetterlund, P. B. *Prog. Polym. Sci.* **2005**, *30*, 605–643.
- (14) Buback, M.; Hippler, H.; Schweer, J.; Vögele, H.-P. *Makromol. Chem., Rapid Commun.* **1986**, *7*, 261–265.
- (15) Beuermann, S.; Buback, M.; Hesse, P.; Junkers, T.; Lacík, I. *Macromolecules* **2006**, *39*, 509–516.
- (16) Gilbert, B. C.; Lindsay Smith, J. R.; Milne, E. C.; Whitwood, A. C.; Taylor, P. J. *Chem. Soc., Perkin Trans.* **1994**, *2*, 1759–1769.
- (17) Buback, M.; Hesse, P.; Lacík, I. *Macromol. Rapid Commun.* **2007**, *28*, 2049–2054.
- (18) Asua, J. M.; Beuermann, S.; Buback, M.; Castignolles, P.; Charleux, B.; Gilbert, R. G.; Hutchinson, R. A.; Leiza, J. R.; Nikitin, A. N.; Vairon, G. J.-P.; van Herk, A. M. *Macromol. Chem. Phys.* **2004**, *205*, 2151–2160.
- (19) Nikitin, A. N.; Hutchinson, R. A. *Macromol. Theory Simul.* **2006**, *15*, 128–136.
- (20) Nikitin, A. N.; Hutchinson, R. A.; Buback, M.; Hesse, P. *Macromolecules* **2007**, *40*, 8631–8641.
- (21) Olaj, O. F.; Kornherr, A.; Vana, P.; Zoder, M.; Zifferer, G. *Macromol. Symp.* **2002**, *182*, 15–30.
- (22) Olaj, O. F.; Kornherr, A.; Zifferer, G. *Macromol. Theory Simul.* **2000**, *9*, 131–140.
- (23) Buback, M.; Egorov, M.; Gilbert, R. G.; Kaminsky, V.; Olaj, O. F.; Russell, G. T.; Vana, P.; Zifferer, G. *Macromol. Chem. Phys.* **2002**, *203*, 2570–2582.
- (24) Buback, M.; Hinton, C. In *High Pressure Techniques in Chemistry and Physics*; Holzapfel, W. B., Isaacs, N. S., Eds.; Oxford University Press: Oxford, U.K., 1997; p 151.
- (25) Kukučková, S. *Ph.D. Thesis, Bratislava/Göttingen*, **2006**.
- (26) Hesse, P. *Unpublished data*, **2007**.
- (27) Beuermann, S.; Buback, M.; Russell, G. T. *Macromol. Rapid Commun.* **1994**, *15*, 351–355.
- (28) Buback, M.; Kuelpmann, A. *Macromol. Chem. Phys.* **2003**, *204*, 632–637.
- (29) Leopold, D.; Fischer, H. *J. Chem. Soc. Perkin Trans. 2* **1992**, *4*, 513–517.
- (30) Fischer, H.; Baer, R.; Verhoolen, R. H. I.; Walbinder, M. *J. Chem. Soc., Perkin Trans.* **1990**, *2*, 787–798.
- (31) Szablan, Z.; Junkers, T.; Koo, S. P. S.; Lovestead, T. M.; Davis, T. P.; Stenzel, M. H.; Barner-Kowollik, C. *Macromolecules* **2007**, *40*, 6820–6833.
- (32) Buback, M.; Kowollik, C.; Kurz, C.; Wahl, A. *Macromol. Chem. Phys.* **2000**, *201*, 464–469.
- (33) Junkers, T. *Ph.D. Thesis, Göttingen*, **2006**.
- (34) Sack-Kouloumbri, R.; Meyerhoff, G. *Makromol. Chem.* **1989**, *190*, 1133–1152.
- (35) Beuermann, S.; Buback, M.; Russell, G. T. *Macromol. Chem. Phys.* **1995**, *196*, 2493–2516.
- (36) Buback, M.; Junkers, T. *Macromol. Chem. Phys.* **2006**, *207*, 1640–1650.
- (37) Schulz, G. V. *Z. Phys. Chem. (Munich)* **1956**, *8*, 290–317.
- (38) Buback, M. *Makromol. Chem.* **1990**, *191*, 1575–1587.
- (39) Buback, M.; Huckestein, B.; Russell, G. T. *Macromol. Chem. Phys.* **1994**, *195*, 539–554.
- (40) Beuermann, S. *Ph.D. Thesis, Göttingen*, **1993**.
- (41) Wako chemicals information brochure.